A high-pressure cell for neutron crystal spectrometry

Buras, B.; Kofoed, W.; Lebech, Bente; Bäckström, G.

Publication date:
1977

Document Version
Publisher's PDF, also known as Version of record

Risø Report No. 357

Risø Report No. 357

Research Establishment Risø

A High-Pressure Cell for Neutron Crystal Spectrometry

by B. Buras, W. Kofoed, B. Lebech and G. Bäckström

April 1977

Sales distributors: Jul. Gjellerup, 87, Sølvgade, DK-1307 Copenhagen K, Denmark

Available on exchange from: Risø Library, Research Establishment Risø, DK-4000 Roskilde, Denmark

UDC 548.78 : 539.893

April 1977 Risø Report No. 357

A HIGH-PRESSURE CELL FOR NEUTRON CRYSTAL SPECTROMETRY

by

B. Buras*, W. Kofoed, and B. Lebech
Physics Department
Research Establishment Risø
DK-4000 Roskilde, Denmark

and

G. Bäckström
Physics Department
University of Umeå
S-90187 Umeå, Sweden

*Also at Physics Laboratory II, University of Copenhagen, Copenhagen, Denmark.

Risø Repro
ISBN 87-550-0456-3

ABSTRACT

Three fixed-scattering-angle methods for neutron scattering powder measurements using double- and triple-axis crystal spectrometers were tested: (1) the analyzer-scan method (AS), (2) the monochromator-scan method (MS), and (3) the monochromator-analyzer scan method (MAS). A high-pressure cell, primarily for use in powder diffraction measurements, with scattering angles of 30°, 60°, 90° and 120° and a sample volume of about 0.8 cm^3 was constructed and used in conjunction with the MS and MAS methods. At room temperature, this cell makes it possible to make measurements at pressures up to about 40 kbar and up to about 30 kbar at 300° C. The report includes a description of the diffraction methods and of the high-pressure cell. A few examples of experimental results are also given.

CONTENTS

1. INTRODUCTION

The construction of high-pressure cells for neutron spectrometry at pressures above 10 kbar began to develop in the mid-sixties when a breakthrough in the technical design was made by Brugger and his collaborators[1-6]. They used the time-of-flight (TOF) diffraction technique[7-9], for which the construction of a pressure cell is somewhat simpler than for more conventional crystal diffractometry. The time-of-flight method uses a pulsed polychromatic incident neutron beam and a fixed scattering angle, and the wave-length distribution of the scattered neutrons is measured by measuring the time needed for the neutron to pass a certain distance. The fixed sample geometry only requires one inlet port and one outlet port. In contrast, the use of a monochromatic incident neutron beam, as in conventional crystal spectrometry, requires a large outlet window for the neutrons diffracted by the sample. Such a window is technically difficult to construct in a pressure cell.

By means of the time-of-flight method Brugger and his collaborators made several neutron diffraction studies[2-6] of powdered crystals at pressures up to 50 kbar. Our work began in 1972[10,11] with the aim of developing simple fixed-scattering-angle neutron diffraction techniques suitable for structural studies of powdered crystals under high pressure and utilizing double- or triple-axis neutron spectrometry.

The diffraction methods tested are outlined in section 2, and their feasibility is illustrated by diffraction patterns of standard samples. The experimental set-up for high pressure studies is described in section 3. Examples of the results of neutron diffraction measurements at high pressures performed with the described equipment are presented in section 4. Section 5 contains a brief discussion.

2. THE DIFFRACTION METHODS

There are three obviously possible fixed-scattering-angle neutron-diffraction powder methods utilizing crystal spectro-

meters: (1) the analyzer-scan (AS) method, (2) the monochromator-scan (MS) method, and the monochromator-analyzer-scan (MAS) method.

2.1. The analyzer-scan method

The AS method shown schematically in fig. 1a is analogous to the TOF method. The incident white neutron beam is scattered by the powdered sample through a fixed angle, $2\theta_o$, and the scattered neutrons are analyzed by means of a single crystal analyzer. Whenever neutrons of wavelength $\lambda_{\underline{H}}$ contained in the incident white beam satisfy the Bragg equation

$$\lambda_{\underline{H}} = 2d_{\underline{HS}}\sin\theta_o \qquad (1)$$

a maximum occurs in the wavelength distribution of the scattered neutrons. In (1) $\underline{H}$ denotes the set of reflection indices (h,k,l), and $d_{\underline{HS}}$ is the interplanar spacing of the sample related to the reflection pertinent to $\underline{H}$.

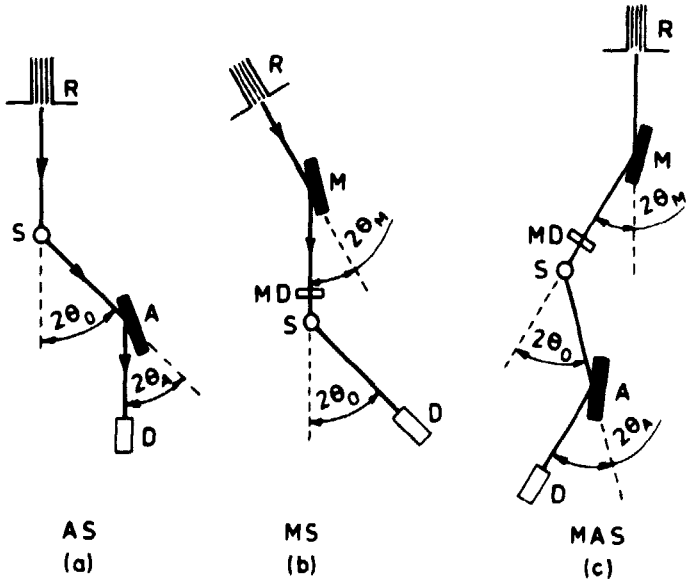

Fig. 1 The principle of the methods proposed for pressure studies: (a) the analyzer-scan method, (b) the monochromator-scan method, and (c) the monochromator-analyzer-scan method. R-reactor, S-powdered sample, M-monochromator crystal, A-analyzer crystal, D-neutron detector, MD-neutron monitor detector.

The scattered neutrons are recorded by the detector when the analyzer single crystal is set in the position defined by the angle $\theta_{\underline{HA}}$ satisfying the Bragg equation

$$\lambda_{\underline{H}} = 2d_A \sin\theta_{\underline{HA}}, \qquad (2)$$

where d_A is the interplanar spacing of the analyzing crystal. By combining (1) and (2) we obtain

$$d_{\underline{HS}} = \frac{d_A}{\sin\theta_o} \sin\theta_{\underline{HA}} = A_o \sin\theta_{\underline{HA}}, \qquad (3)$$

where $A_o = d_A/\sin\theta_o$ is a constant for the particular experimental set-up. Thus, once the Bragg angle $\theta_{\underline{HA}}$ is determined in an analyzer-scan, we can deduce the interplanar $d_{\underline{HS}}$ by means of (3).

In general, it should be noted that in (3), A_o and $d_{\underline{HS}}$ should be replaced by $A_n = A_o/n$ and $d^{(n)}_{\underline{HS}}$, where n is the order of the analyser reflection. Thus in addition to the peaks observed in more conventional powder diffraction patterns, higher-order peaks may be expected. The appearance of higher-order reflections is also relevant in the MS and MAS methods described below.

We tested the AS method using a double-axis crystal spectrometer at the DR 3 reactor at Risø. The sample was placed on the monochromator table and the analyzer crystal on the sample table. Figure 2a shows a section of a neutron diffraction pattern obtained for a Si powder by means of the AS method ($2\theta_o = 90^o$) using the (1,1,1) reflection from a Ge crystal as analyzer. No higher-order reflections are observed because the second-order reflection is forbidden in the diamond structure and the third-order of the maximum wavelength (2.72 Å) is rather weak.

2.2. The monochromator-scan method

In the MS method the incident neutron beam is monochromatic, but its wavelength is continuously changed (in practice stepwise) by altering the Bragg angle $\theta_{\underline{HM}}$ of the monochromator. The

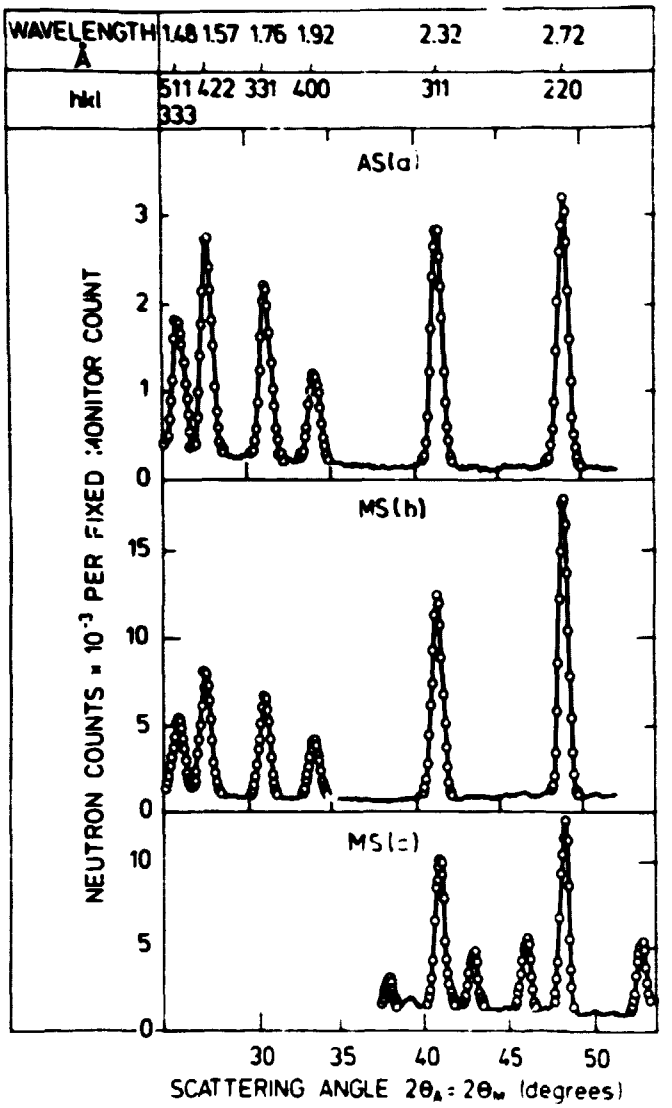

Fig. 2 Sections of neutron diffraction patterns from powdered Si obtained by means of the analyzer-scan method (a) and the monochromator-scan method (b and c) for a fixed scattering angle of 90°. In a and b the analyzer or monochromator was the (1,1,1) reflection from Ge. As monochromator in (c) was used the (0,0,2) reflection from pyrolytic graphite.

arrangement is shown schematically in fig. 1b. The detector records a peak whenever the following condition is fulfilled

$$d_{\underline{HS}} = \frac{d_M}{\sin\theta_o} \sin\theta_{\underline{HM}} = M_o \sin\theta_{\underline{HM}}, \qquad (4)$$

where $M_o = d_M/\sin\theta_o$ is a constant for a particular set-up, and d_M is the interplanar spacing of the monochromator crystal.

The MS method requires a double-axis crystal spectrometer with a continuously variable wavelength of the monochromatic beam. Figure 2b shows a section of a neutron pattern of Si powder obtained by this method ($2\theta_o = 90^o$) using the (1,1,1) reflection from a Ge crystal as monochromator. As in fig. 2a, no additional higher-order peaks are visible. Figure 2c shows a section of a neutron pattern of the same Si sample obtained using the (0,0,2) reflection from a pyrolytic graphite crystal as monochromator. Second-order peaks arising from the (0,0,4) reflection in graphite are clearly visible.

2.3. The monochromator-analyzer-scan method

The MAS method combines the two methods outlined above. The arrangement is shown schematically in fig. 1c. From (3) and (4) we have

$$d_{\underline{HS}} = \frac{d_A}{\sin\theta_o} \sin\theta_{\underline{HA}} = \frac{d_M}{\sin\theta_o} \sin\theta_{\underline{HM}} \qquad (5)$$

and thus the angle $\theta_{\underline{HA}}$ must follow the angle $\theta_{\underline{HM}}$ in such a way that

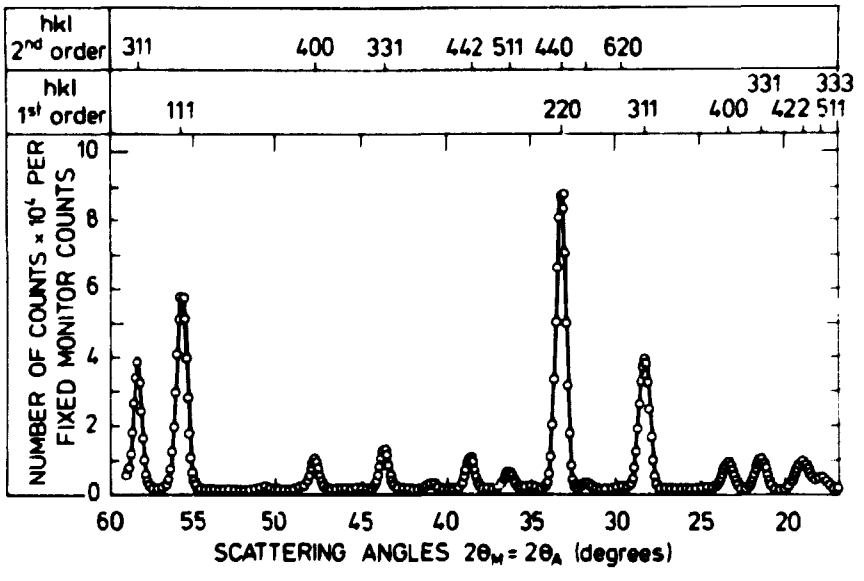

Fig. 3 A section of a neutron diffraction pattern of powdered silicon obtained by means of the monochromator-analyzer-scan method. The (0,0,2) reflection from pyrolytic graphite is used as both monochromator and analyzer ($2\theta_o = 90^o$).

$$d_A \sin\theta_{\underline{HA}} = d_M \sin\theta_{\underline{HM}}. \qquad (6)$$

For $d_A = d_M$, we get $\theta_{\underline{HA}} = \theta_{\underline{HM}}$ implying that the analyzer and the monochromator should be turned by equal angles. The MAS method requires a triple-axis spectrometer with a continuously variable neutron wavelength. Figure 3 shows a section of a monochromator analyzer scan obtained for the standard Si sample. Both the analyzer and the monochromator are pyrolytic graphite. The fixed scattering angle is 60°. As in fig. 2c, higher-order reflections are clearly visible.

3. THE HIGH-PRESSURE EXPERIMENTAL ARRANGEMENT

The high-pressure cell is of the same type as that used by Brugger et al.[1]. The centre part of the cell is shown in fig. 4. It consists of a housing made from an aluminium oxide cyl-

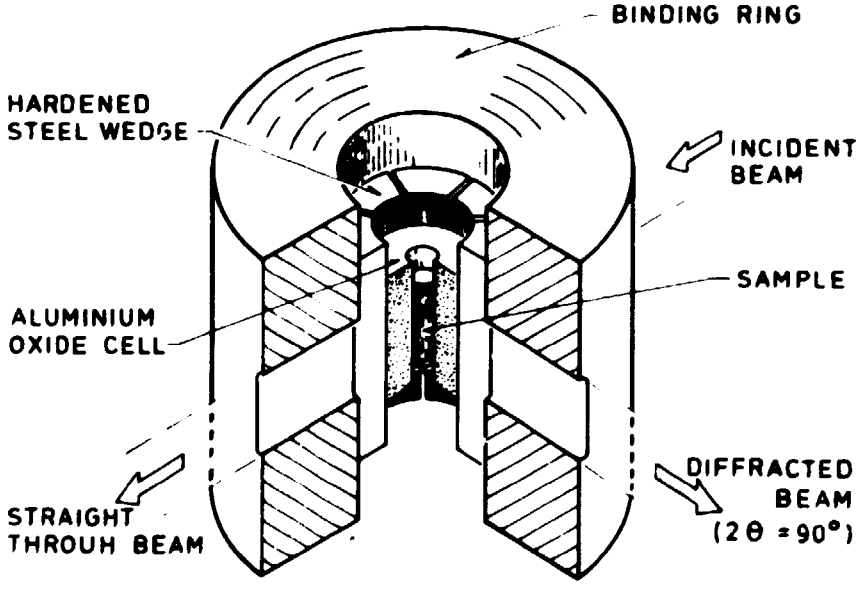

Fig. 4 Centre part of the high-pressure cell (perspective view).

inder, 6.3 cm high, 3.2 cm in diameter and with a 0.64 cm bore. The cell is supported by hardened steel wedges and these are supported by a binding-ring. The aluminium oxide has a high compressive strength, but a low tensile strength. It is loaded by pre-pressing with a force of about 20 tons. This ensures

that the aluminium oxide is within the tensile strength, even when the sample is at high pressure. The steel wedges are 30° segments of a cylinder so that there are 0.34 cm wide gaps every 30°. There are a number of similar gaps, 0.34 cm wide and 2.4 cm high, in the supporting binding-ring, and these make possible the use of scattering angles of 30°, 60°, 90°, and 120°. Tungsten carbide pistons transmit the force from two

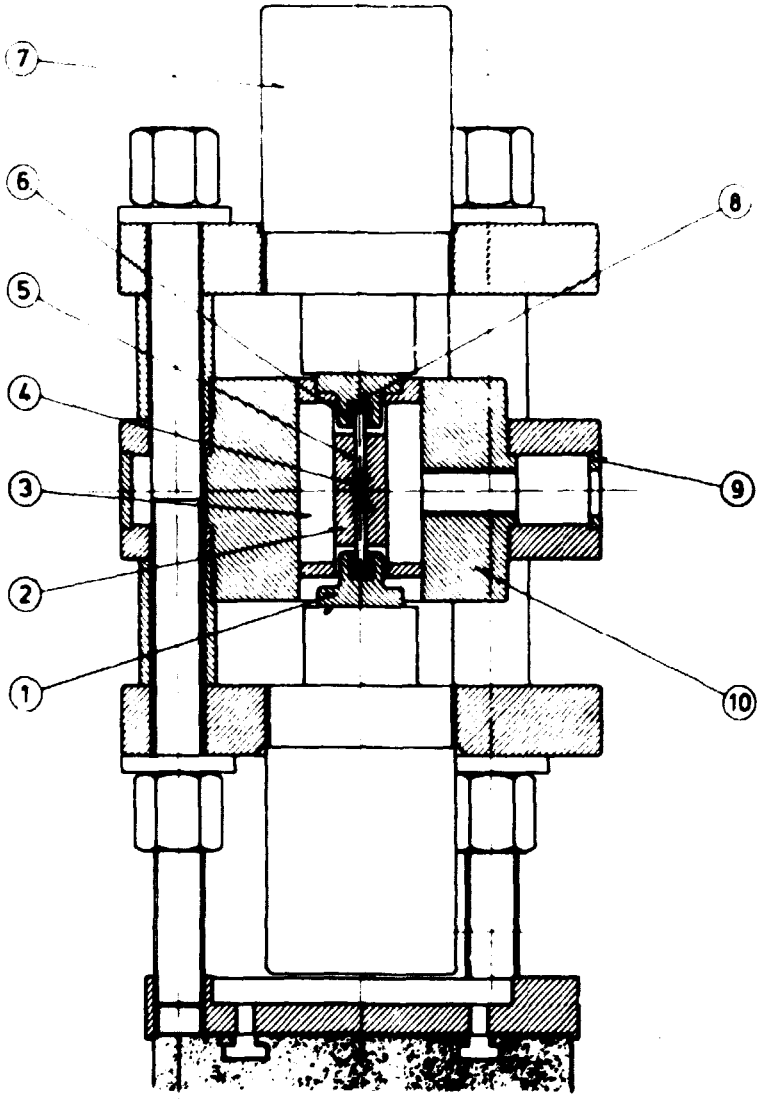

Fig. 5 Principle drawing of the high-pressure set-up. 1) Piston shoe. 2) Aluminium oxide cell. 3) Hardened steel wedges. 4) Sample. 5) Tungsten carbide piston. 6) Brass wedge. 7) Hydraulic ram. 8) Piston support. 9) Cadmium shield with diaphragms. 10) Binding ring.

0.3 MN hydraulic rams to the sample (fig. 5). In the first design, flat piston shoes were used (1 in fig. 5) and the alignment of the pistons was very critical. A slight misalignment led to the breakage of the pistons at pressures of about 25-30 kbar. In an improved design spherical piston shoes (fig. 6)

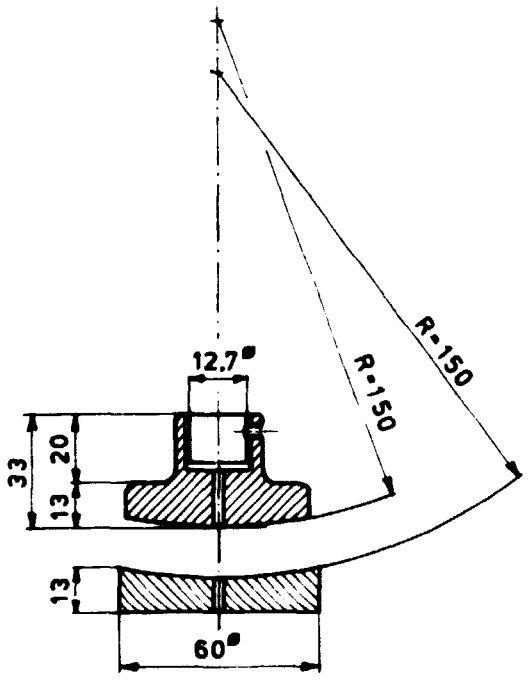

Fig. 6 Spherical piston shoes.

ensure alignment of the pistons. With this design the maximum pressure is usually above 40 kbar before piston breakage occurs.

The sample is enclosed in a thin walled (0.04 cm) cylindrical teflon (polytetrafluorethylene) container sealed at both ends by teflon plugs. In order to obtain semihydrostatic pressure, the powder has been wetted in some cases by adding carbon disulphide (CS_2) or fluorinert FC-75 (from 3 M). For high-temperature measurements, a resistance wire is wound around the teflon container and the electrical current is supplied through the tungsten carbide pistons. The temperature is determined by measuring the power supplied to the electrical heater using a calibration of the heater power (at 6 kbar and 10 kbar) versus temperature obtained in a separate experiment. This indirect determination of temperature had to be adopted because the copper-konstantan thermocouples, used to measure the temperature, broke at high pressures. Improved control carried out by means

of a thermocouple inside the sample at all pressures is now being constructed. With the present set-up we can heat the sample to about 570 K at 30 kbar.

The cell pressure is calibrated with respect to the oil pressure of the hydraulic ram by utilizing the pressure-induced anomaly in the electrical resistivity and/or the changes of crystallographic structure of Ce and Bi, as observed by neutron diffraction, when passing the well known phase transitions. For the resistivity measurements, a Bi or Ce wire is placed inside the teflon container and the tungsten carbide pistons provide the electrical contacts to both ends of the wire. At pressures between the known transition points, we assume a linear relationship between the pressure inside the cell and the oil pressure. The reproducibility of this calibration is satisfactory. At 7.5 kbar, the differences amount to less than 0.5 kbar and at 25 kbar to less than 1 kbar.

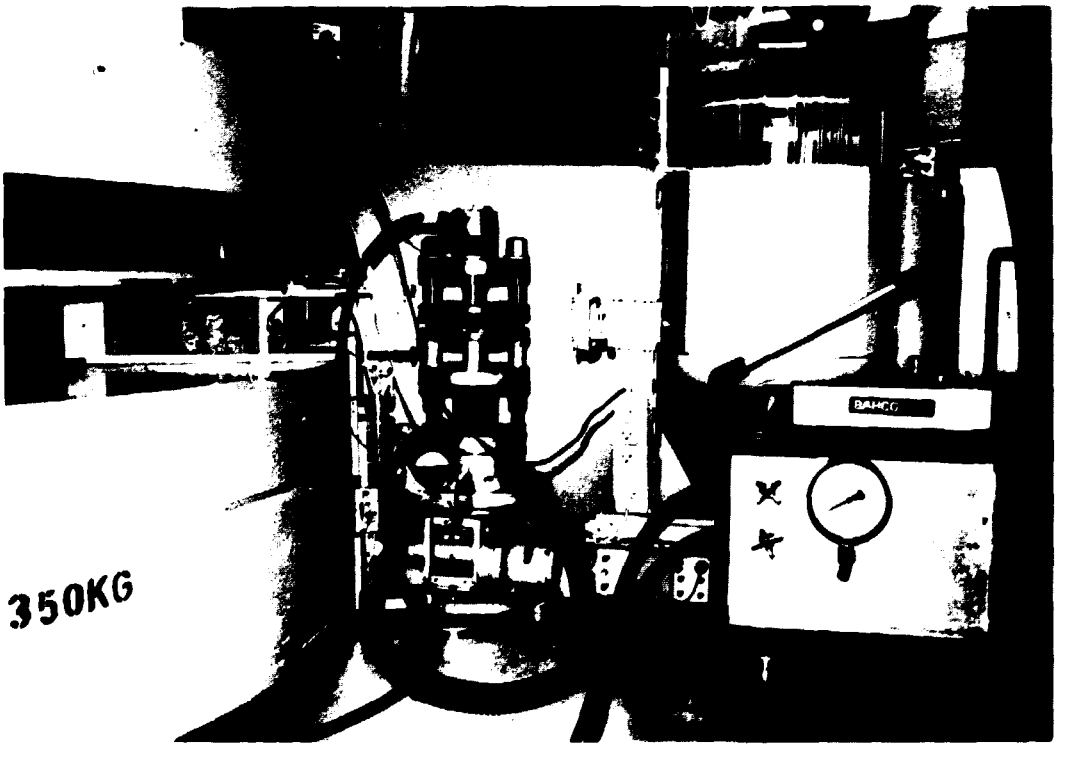

Fig. 7 The high-pressure set-up on the sample table of the TAS IV neutron triple-axis crystal spectrometer at the DR 3 reactor at Risø.

4. EXAMPLES OF RESULTS OF NEUTRON DIFFRACTION MEASUREMENTS AT HIGH PRESSURES

The first test experiments were carried out on polycrystalline Bi. At atmospheric pressure Bi is rhombohedral, BiI. The unit cell is defined by a = 4.736 Å and $\alpha = 57.233^{\circ}$ [12]. At 25.3 kbar BiI transforms to BiII. According to Brugger et al.[3], BiII is monoclinic with a unit cell defined by a = 6.674 Å, and b = 6.117 Å, c = 3.304 Å, and $\beta = 110.38^{\circ}$. At 26.8 kbar, BiII changes to BiIII. Neutron diffraction patterns of BiIII were obtained by Brugger et al.[6]. The interplanar spacings were reported, but no unit cell was assigned to BiIII.

Our experiments[11] were carried out at one of the triple-axis spectrometers using both the monochromator-scan method and the monochromator-analyzer-scan method. (Spatial limitations prevented the test of the analyzer-scan method in conjunction with the high pressure equipment). Figure 7 shows the high pressure cell placed on the sample table of the spectrometer. The positions of all spectrometer arms and tables are controlled by a PDP 8 computer and can be changed in small steps. The monochromatic neutron beam is monitored by a fission detector placed at the outlet of the monochromator-sample collimator. All measurements were performed for a constant number of monitor counts. The diffracted neutrons are detected by a He^3 neutron detector. The collimation is defined by the width of the sample, and this limits the scattering from the aluminium oxide cell and from the tungsten carbide pistons to multiple scattering. This is illustrated in the diffraction patterns (figs. 8-10) by the absence of Bragg peaks other than those arising from the sample.

Figure 8a shows the neutron diffraction pattern of BiI at 5.5 kbar obtained in the present study by means of the MS method using a pyrolytic graphite monochromator and a 90° scattering angle. A rather high background is noticed. For comparison, fig. 8b shows the neutron pattern of BiI at atmospheric pressure obtained by means of the MAS method using pyrolytic graphite as both monochromator and analyzer ($2\vartheta = 90^{\circ}$). A dramatic

improvement of the peak-to-background ratio as compared to that of fig. 8a is easily observed.

In fig. 9 the diffraction patterns of bismuth at atmospheric pressure (BiI), 26 kbar (BiII), and 30 kbar (BiIII) are compared. The patterns were obtained by means of the MAS method using a scattering angle of 60°. All these diffraction pat-

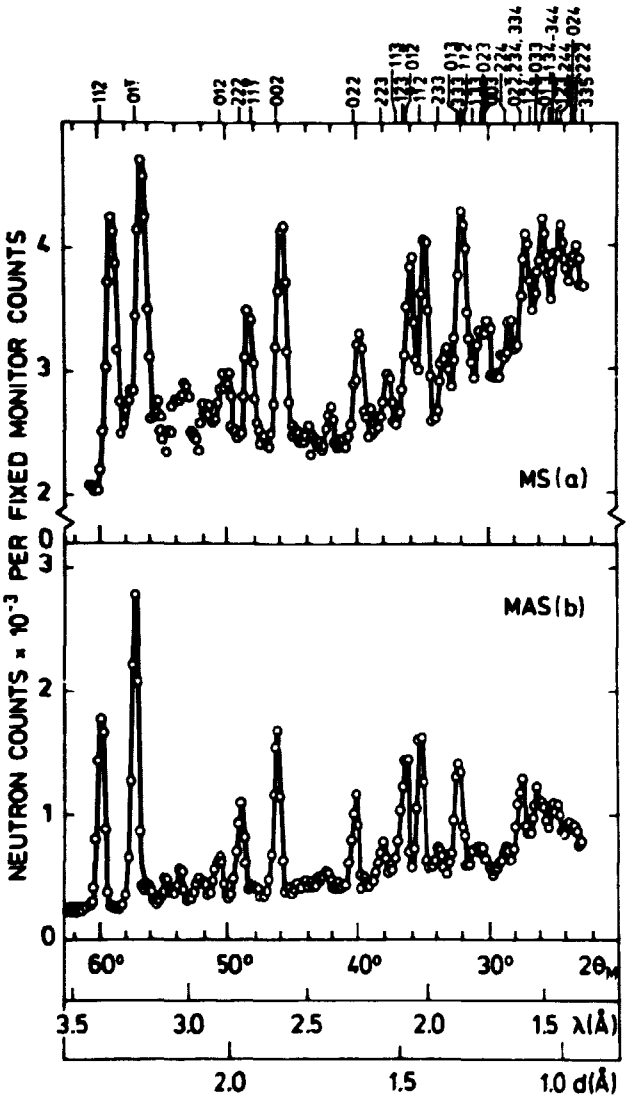

Fig. 8 Neutron diffraction patterns of BiI obtained for a fixed scattering angle of 90° using pyrolytic graphite crystals as monochromator and analyzer.
(a) BiI at 5.6 kbar using the MS method.
(b) BiI at 1 atm using the MAS method.
The positions of the Bragg reflections at 1 atm are marked at the top of the diagram.

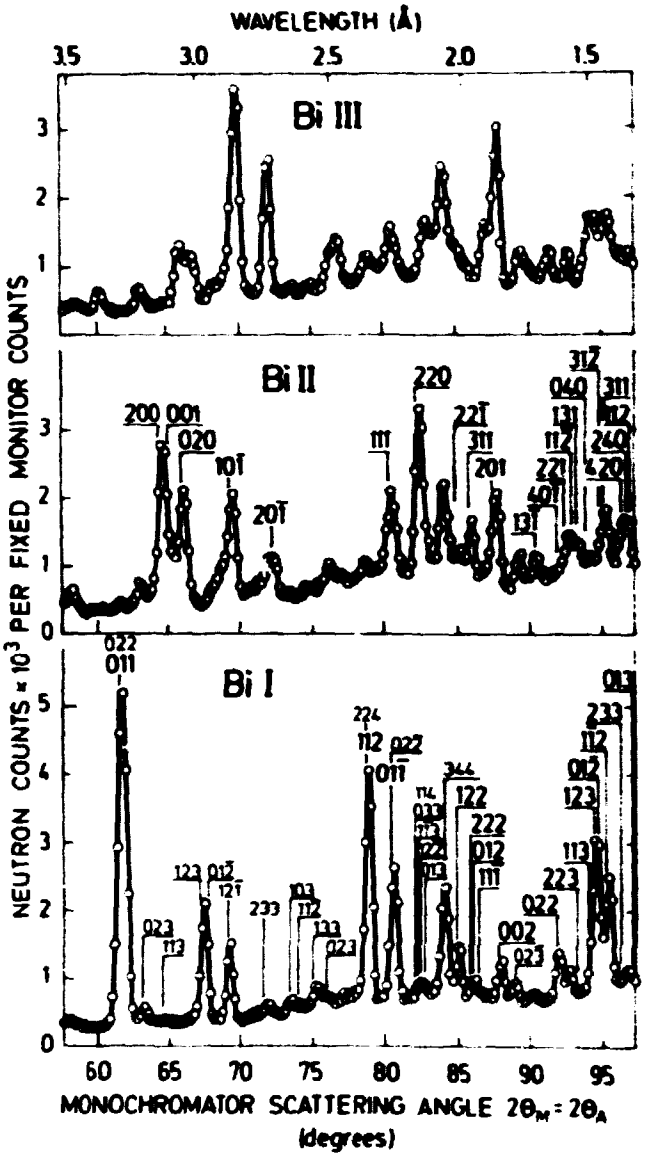

Fig. 9 Neutron diffraction patterns of Bi at 1 atm, 26 kbar, and 30 kbar, obtained as in fig. 8, but for a fixed scattering angle of 60°. (Rhombohedral indices).

terns were obtained in less than 30 hours depending somewhat on the desired statistics and the angular steps of the spectrometer arms. The diffraction pattern obtained for BiIII at 30 kbar is shown in more detail in fig. 10. The peaks are numbered as done by Brugger et al.[6] (first-order peaks by large numbers, second-order peaks by smaller numbers). The interplanar spacings deduced from fig. 10 are compared with those measured by Brugger et al.[6] in table 1. The agreement between the peaks observed in both cases is satisfactory; however, a unit cell cannot be fitted to Brugger's or to our data, and so

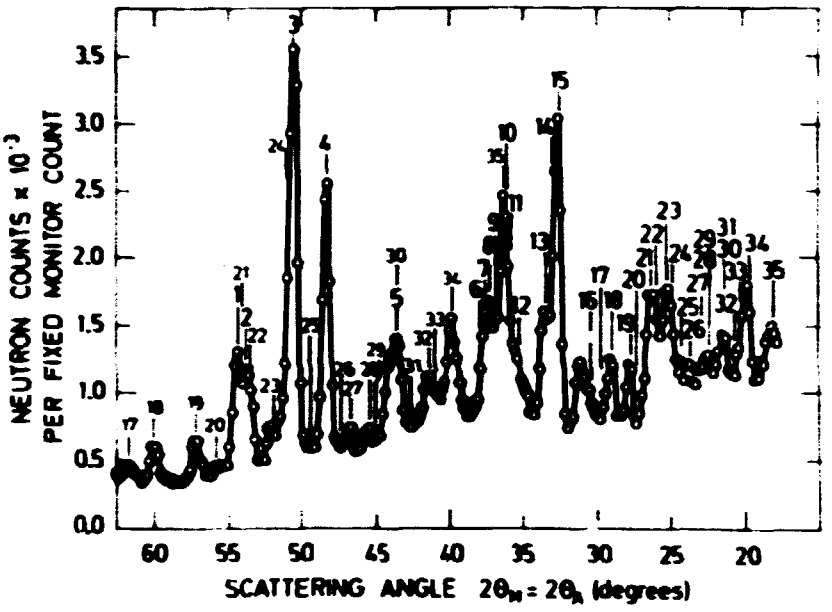

Fig. 10 Neutron diffraction pattern of BiIII at 30 kbar obtained as in fig. 9. The peaks are numbered as in Brugger et al.[6], large numbers signify the first-order Bragg peaks, the smaller numbers the second-order peaks.

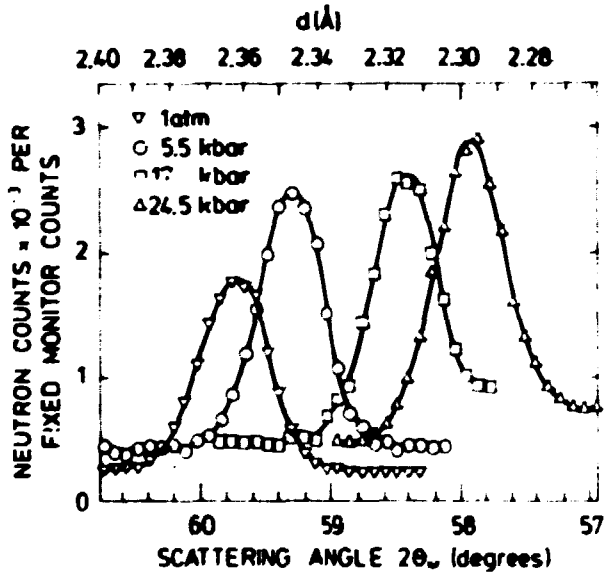

Fig. 11 Shift with pressure of the (1,1,2) reflection of BiI obtained as in fig. 10. (Rhombohedral incides).

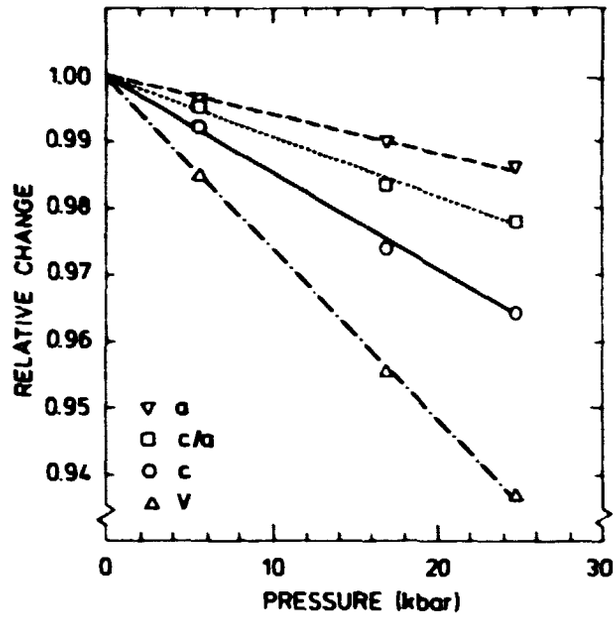

Fig. 12 Relative pressure dependence of the hexagonal unit cell dimensions or unit cell volume for BiI.

the structure of BiIII remains an unsolved question. For BiI, the pressure dependence of the unit cell dimensions may be determined from the observed shifts of the (1,1,2) (fig. 11) and the (0,1,1) reflections. The relative pressure dependence of the unit cell dimensions and the unit cell volume is shown in fig. 12.

The same cell and the MAS method were used for other phase transformation studies, e.g. of TeO_2 (paratellurite)[13,14], benzene[15], naphtalene[15], SnI_4[16], and Ce metal[17]. For illustration purposes, we briefly describe the TeO_2 and Ce results.

Figure 13 shows sections of neutron diffraction patterns of TeO_2 at 300 K and at atmospheric pressure, 14.5 kbar, and 22 kbar. The splitting of the (0,1,2) and (1,2,2) Bragg peaks, because of the second-order structural phase transition at 9 kbar from a tetragonal to a orthorhombic structure[13,14,18-20], is more pronounced in our diffraction patterns than in those obtained by means of the TOF method[19].

In the case of Ce metal[17], the pressure-volume isotherms were measured on going through the γ to α isomorphic first-order

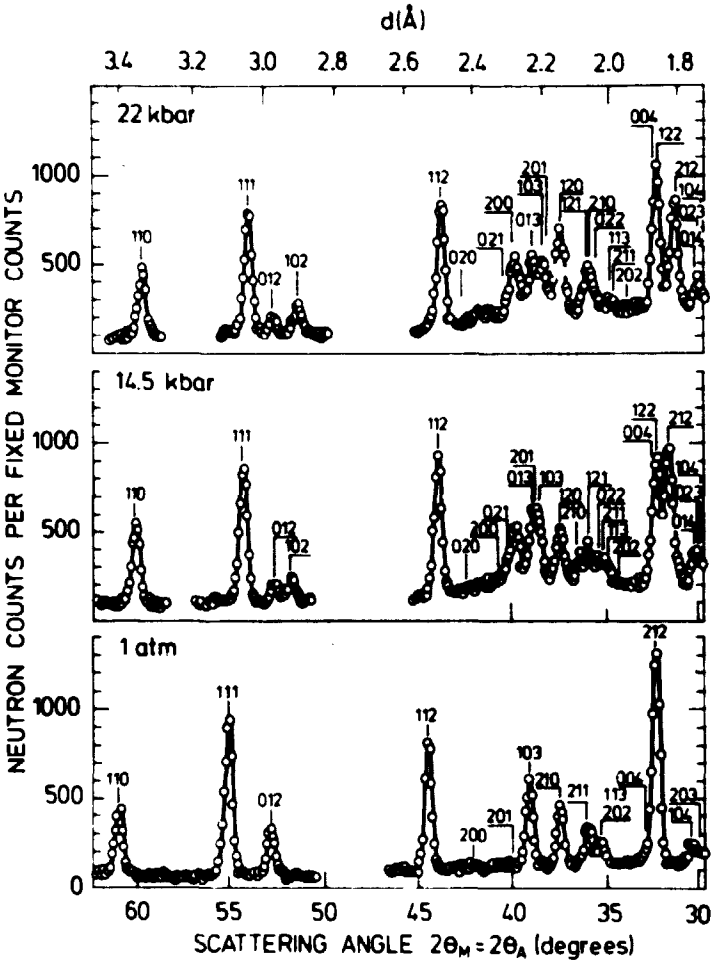

Fig. 13 Neutron diffraction patterns of TeO_2 at 1 atm, 14.5 kbar, and 22 kbar. Notice the splitting of the (0,1,2) and (2,1,2) peaks due to a structural phase transformation at 9 kbar from a tetragonal to an orthorhombic structure.

transition up to 550 K at 27 kbar. The experimental points in fig. 14 represent the temperature dependence of the densities of the γ-Ce, and α-Ce. The data were obtained by first adjusting the temperature to a suitable value and then adjusting the pressure to the value at which the two phases were simultaneously present. This enabled precise measurements of volume (density) changes. The volume of the unit cell of Ce at each temperature and pressure was calculated from the measured position of the (1,1,1) Bragg reflection. At temperatures close to the critical point, the (1,1,1) reflections from the two phases overlap. Therefore, the peak positions were determined from a least squares fit of the measured line-shape to a sum of two Gaussians. Using the unit cell volume deduced from the peak positions, the critical temperature and the critical exponent

β were determined from a least squares fit of T_c, β, and C to the equation

$$\Delta\rho(T) = \rho_\alpha(T) - \rho_\gamma(T) = C(1-T/T_c)^\beta .$$

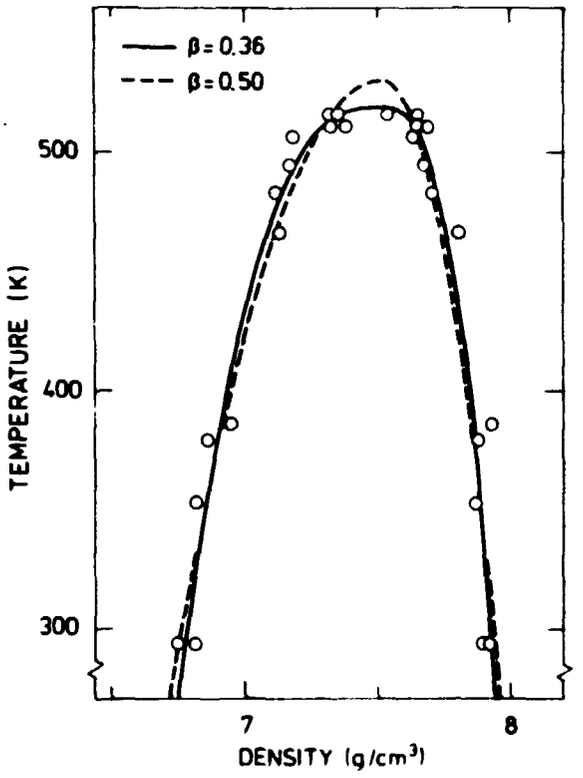

Fig. 14 Temperature versus density (T,ρ) for Ce-metal. The solid line is a two-parameter fit as described in the text. The dashed line is a one-parameter fit with fixed β = 0.5.

Leaving all three parameters free to vary, one obtains β = 0.36 and T_c = 519 K (solid line in fig. 14). Another fit with β = 0.5 yields T_c = 530 K (dashed line in fig. 14), which implies that with the resolution used two partly overlapping (1,1,1) peaks should be observed close to, but above 519 K. However, when increasing the temperature from 519 K, where the two peaks can be resolved, to 521 K a rapid coalescence of the two peaks into one with almost no broadening was observed. This confirms that $\beta \sim 0.36$ and 519 K < T_c < 521 K. The measurement will be repeated with the improved temperature control mentioned in section 3.

Although the cell was constructed for powder diffraction measurements, it can be used for single crystals too. We utilize the

fact that with a fixed scattering-angle a wavelength scan is a scan along a straight line in the reciprocal space. This application is illustrated by a study of the pressure dependence of the Néel temperature of Cr single crystals[14]. A cylindrical Cr single crystal (5.5 mm in diameter, 15 mm long) was mounted in the cell with the [001] zone axis vertical and parallel to the cylinder axis. By turning the crystal around the zone axis, the crystal was oriented using the strong (2,0,0) nuclear reflection, and by means of a monochromator scan the magnetic satellite reflections (1+Q,0,0) and (1-Q,0,0) were recorded as shown in the insert of fig. 15. The temperature dependence of

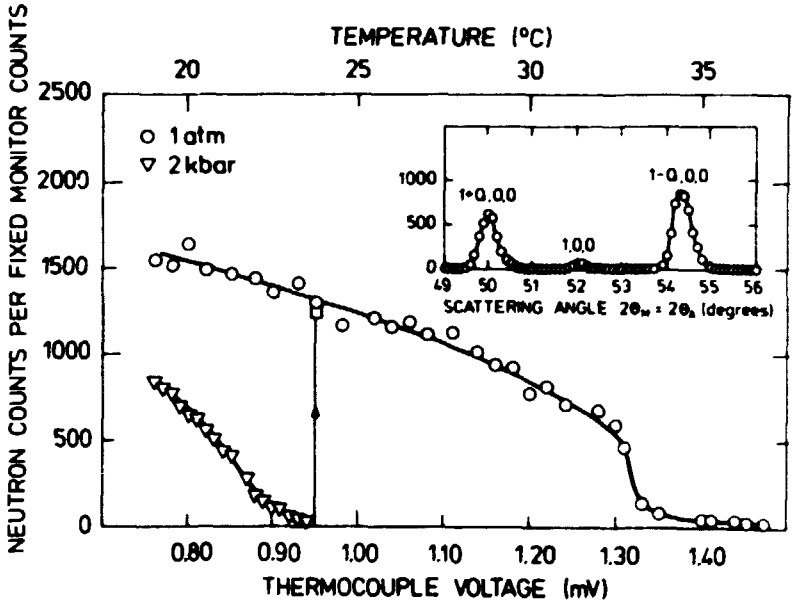

Fig. 15 Intensity of the (1-Q,0,0) magnetic satellite as function of temperature for 1 atm (o) and 2 kbar (Δ). When the pressure is released at 23.8° C, the intensity jumps to the value shown by the square (□). The insert is a neutron diffraction pattern showing the magnetic satellites of (1-Q,0,0) and (1+Q,0,0); the small 100 reflection is a second-order contamination.

the intensity of the (1-Q,0,0) magnetic satellite was measured at atmospheric pressure and at 2 kbar (fig. 15). As can be seen, the Néel temperature decreases by (9.5±1) K upon increasing the pressure from 1 atm to 2 kbar, in agreement with other measurements[22,23].

For measurements of larger samples under pressures up to about 8 kbar, we constructed a cell with a 360° window from a high-

strength heat-treatable alloy B26S/WP, which replaced that shown in fig. 4. The set-up with this cell is shown in fig. 16. The cylindrical specimen is 15 mm in diameter and 60 mm long. The pressure is applied via hardened steel pistons driven by rams with oil at pressures up to 400 atmospheres, as in the previously described cell. This cell can be used for conven-

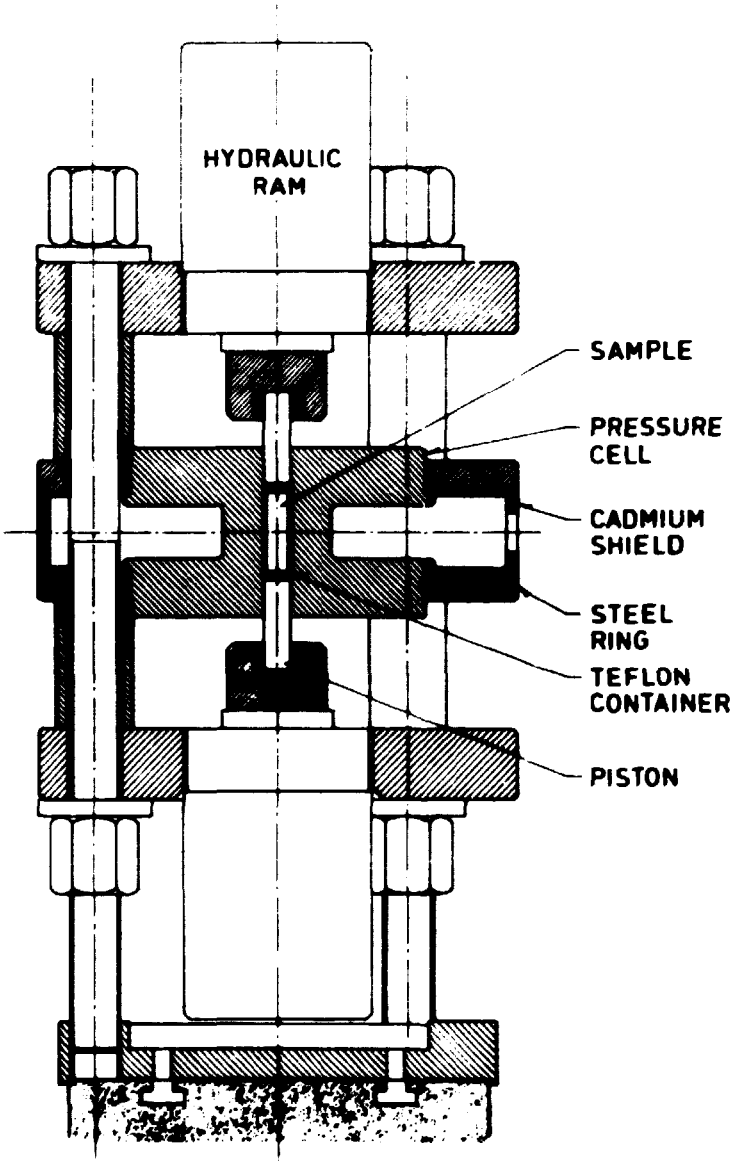

Fig. 16 The high-pressure set-up with a large volume cell made from a high tensile strength alloy.

tional diffractometry. It was used for studies of inelastic neutron scattering from Ce metal[24] at room temperature both below and above the previously mentioned γ to α phase transition. It was found that (a) there is no indication of any residual magnetic scattering in the collapsed α phase, and (b)

the energy width of the paramagnetic scattering in the γ phase increases with pressure.

5. DISCUSSION

It follows from our measurements that the monochromator-analyzer-scan method is superior to the other two methods described above. Using the MAS method, we record only the neutrons elastically scattered by the sample and the peak-to-background ratio is very favourable. The second feature is partly a consequence of the first and partly caused by the fact that the detector does not directly see the high pressure cell, which naturally gives a lot of scattering. Although an analyzer crystal reduces the recorded intensity, the reduction is negligible when pyrolytic graphite is used as analyzer and monochromator. If, however, use is made of a Ge analyzer in order to avoid second-order contaminations and a pyrolytic graphite monochromator, the intensity decreases by a factor of 3-4 as compared with use of the graphite analyzer.

The peak-to-background ratio in the MAS method is better than in the TOF method; however, the disadvantage of the MAS method, as compared with the TOF method, is that the Bragg peaks are recorded one after another while in the TOF method all peaks are recorded at the same time. Thus, demands for stability with time of pressure and temperature are greater when using the MAS method. On the other hand, whenever desirable, the measurements may be concentrated on one or a few representative peaks, which may be measured with high resolution and/or high statistical accuracy, as, for example, in the case of TeO_2 (fig. 13), where only the relevant parts of the diffraction patterns were measured.

As in the TOF method, the resolution is better for large interplanar spacings than for small ones, in contrast to the resolution found in conventional double-axis spectrometry. This is illustrated by the examples shown in fig. 17 for a graphite monochromator. For the fixed-scattering-angle methods the range of measurable interplanar spacings d decreases with increasing

scattering angle $2\theta_o$. Thus, if the intensity is sufficient in the wavelength range from $\sim$ 1 Å to 4.5 Å, (which is the case for most thermal neutron beams) the available ranges of interplanar placings are:

$$2\ \text{Å} \lesssim d \lesssim 8.7\ \text{Å} \quad \text{for } 2\theta_o = 30^o,$$
$$1\ \text{Å} \lesssim d \lesssim 4.5\ \text{Å} \quad \text{for } 2\theta_o = 60^o, \text{ and}$$
$$0.7\ \text{Å} \lesssim d \lesssim 3.2\ \text{Å} \quad \text{for } 2\theta_o = 90^o.$$

From inspection of fig. 17 it follows that, to a good approximation, the resolution defined as $\frac{\Delta d}{\Delta\theta_M}$ equals

$$R \sim \frac{\Delta d}{\Delta\theta_M} \approx \frac{d_M \sin 45^o}{45^o \times \sin\theta_o} \quad \text{for } \theta_M \leq 45^o$$

The condition on θ_M is fulfilled in normal crystal diffractometry, which implies that the resolution is almost indepen-

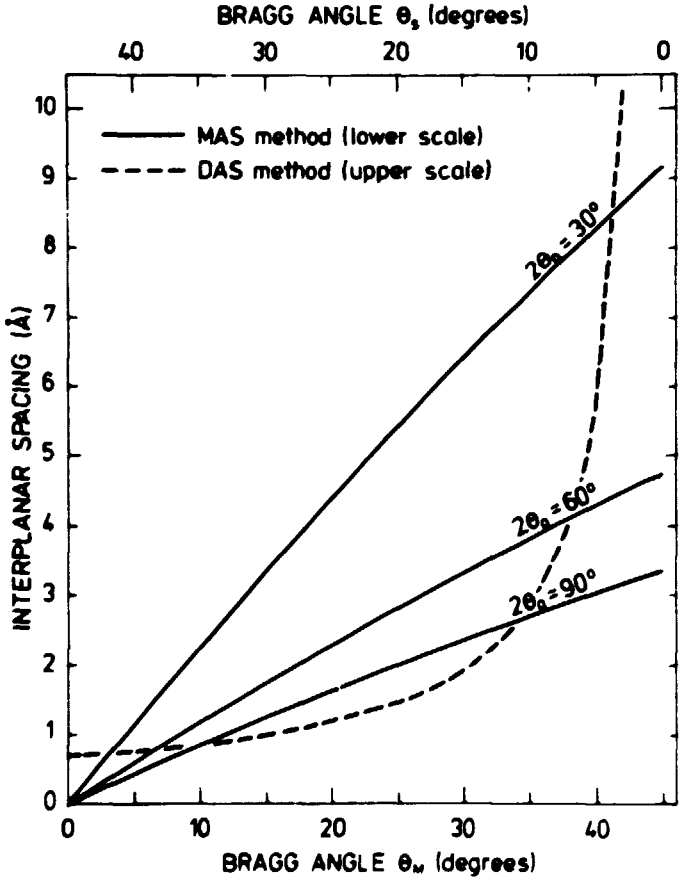

Fig. 17 Resolutions calculated for the monochromator-analyzer-scan method (MAS) and for conventional double-axis spectrometry (DAS).

dent of the lattice spacing. Thus, in fig. 17, the θ_M-axis is approximately a d-axis. The resolution improves with increasing scattering angle. For a graphite monochromator ((0,0,2) reflection), we find

$$R \sim 0.2 \text{ Å/deg} \quad \text{for } 2\theta_o = 30^o,$$
$$R \sim 0.1 \text{ Å/deg} \quad \text{for } 2\theta_o = 60^o, \text{ and}$$
$$R \sim 0.07 \text{ Å/deg} \quad \text{for } 2\theta_o = 90^o.$$

The dashed line in fig. 17 shows the dependence of d on the Bragg angle θ_s at $\lambda = 1$ Å for a conventional double-axis spectrometer. R increases with increasing d-spacing, i.e. the resolution gets poorer.

The full widths at half maximum (FWHM) of the diffraction peaks may be freely adjusted by proper collimation. A neutron diffraction pattern covering interplanar spacings from 1.5 Å to 3.5 Å may at $2\theta_o = 60^o$ be obtained in $\sim$ 24 hours with reasonable statistics and a FWHM equal to 1^o. (See, for instance, one of the patterns in fig. 9).

Whenever present, the higher-order Bragg peaks from the sample are a disturbing factor in the case of low-symmetry crystals. However, in the case of high-symmetry crystals, where overlapping peaks are not so common, the higher-order peaks may supply additional information. Although the structure factors may in principle be deduced from the integrated intensities of the peaks measured by the MAS method, some problems still remain unsolved. The incident neutron spectrum may be measured by a monitor in the beam (with proper corrections for the higher-order contamination of this beam); but to determine reliable structure factors, consideration must also be given to the reflectivity of the analyzer crystal - in addition to absorption in the pressure cell. Several calibration methods were tested, but all were unsatisfactory, especially for wavelengths below 1.8-2 Å, and work continues on the solution of this important problem.

While we were working on our fixed-scattering-angle pressure cell, McWhan et al.[21] constructed a high-pressure cell with

large windows for elastic and inelastic neutron scattering experiments with both powdered and single crystals that is capable of working up to 50 kbar. An incident monochromatic neutron beam is used and the peaks are recorded as in conventional double-axis spectrometry. This cell seems to be more versatile than ours, but the neutron patterns show numerous aluminium oxide peaks from the cell, while in our case there are no aluminium oxide peaks at all because of the fixed-scattering-angle geometry.

After several years of experience, we conclude that our high-pressure cell and the monochromator-analyzer-scan method make possible neutron diffraction studies of powdered samples at pressures up to about 40 kbar at room temperature and up to about 30 kbar at about 570 K. The method is simple and especially suitable for measurements of interplanar spacings, while structure factor determination still needs some improvements.

ACKNOWLEDGMENTS

One of us (W.K.) would like to thank Mr. J.B. Savin, A.W.R.E. Aldermaston, England, and Mr. D.G. Prince, J.J. Thomson Laboratory, University of Reading, England for useful discussions concerning the construction of the high pressure cell.

Table 1 Interplanar spacings of BiIII

Peak number	This study	Brugger et al.[6]
1	3.065	3.072
2	3.032	3.034
3	2.867	2.865
4	2.747	2.745
5	2.490	2.492
6		2.189
7		2.170
8	2.154	2.156
9		2.124
10	2.089	2.087
11		2.068
12		2.015
13	1.933	1.935
14		1.908
15	1.882	1.885
16		1.762
17	1.721+	1.725
18	1.679•	1.679
19	1.602•	1.602
20	1.570+	1.584
21	1.515	1.526
22		1.509
23	1.471•	1.471
24		1.444
25	1.402	1.393
26	1.371	1.360
27	1.328+	1.328
28	1.296•	1.295
29		1.287
30	1.245	1.247
31		1.223
32	1.188+	1.196
33		1.175
34	1.142•	1.142
35	1.050	1.050

•Based on first and second order reflections

+Based on second order reflections only

REFERENCES

1. R.M. Brugger, R.B. Bennion, T.G. Worlton, and E.R. Peterson, Neutron Diffraction Studies of Samples at High Pressures. IDO-17170 (1966) 55 pp.
and in: Research Applications of Nuclear Pulsed Systems. Proceedings of a Panel held in Dubna, USSR, 18-22 July, 1966. (IAEA, Vienna, 1967) 35-61.

2. T.G. Worlton, R.B. Bennion, R.M. Brugger, Pressure Dependence of the Morin Transition in α-Fe_2O_3 to 26 kbar. Phys. Lett. 24A (1967) 653-655.

3. R.M. Brugger, R.B. Bennion, and T.G. Worlton: The Crystal Structure of Bismuth-II at 26 kbar. Phys. Lett. 24A (1976) 714-717.

4. T.G. Worlton, R.M. Brugger, and R.B. Bennion, Pressure Dependence of the Néel Temperature of Cr_2O_3. J. Phys. Chem. Solids 29 (1968) 435-438.

5. T.G. Worlton and D.L. Decker, Neutron Diffraction Study of the Magnetic Structure of Hematite to 41 kbar. Phys. Rev. 171 (1968) 596-599.

6. R.M. Brugger, R.B. Bennion, T.G. Worlton, and W.R. Myers, Neutron Diffraction at High Pressures. Trans. Am. Crystallogr. Assoc. 5 (1969) 141-154.

7. B. Buras and J. Leciejewicz, A Time-of-Flight Method for Neutron Diffraction Crystal Structure Investigations. Nukleonika 8 (1963) 75-77.

8. K.C. Turberfield, Time-of-Flight Neutron Diffractometry. In: Thermal Neutron Diffraction. Proceedings of the International Summer School at Harwell, 1-5 July 1968 on the Accurate Determination of Neutron Intensities and Structure Factors. Edited by B.T.M. Willis. (Oxford University Press, London, 1970) 34-50 and references therein.

9. B. Buras, Time-of-Flight Diffractometry. In: RCN-234 (1975) 307-346, and references therein.

10. B. Buras, B. Lebech, and W. Kofoed, Structure Studies under High Pressure. In: Risø Report No. 288 (1973) 32-33.

11. B. Buras, B. Lebech, W. Kofoed, and G. Bäckström, Structure Studies under High Pressures. In: Risø Report No. 300 (1973) 44-45.

12. W.B. Pearson, "Handbook of Lattice Spacing and Structures of Metals and Alloys", Vol. 2. (Pergamon Press, Oxford, 1967) 81.

13. S. Shapiro, B. Buras, W.D. Ellenson, and T. Giebultowicz, Pressure-Induced Phase Transition in TeO_2. In: Risø Report No. 320 (1974) 56-57.

14. B. Buras, W.D. Ellenson, B. Lebech, and S.M. Shapiro, High Pressure Neutron Diffraction Studies of Structural and Magnetic Phase Transformations. In: Electronic Properties of Solids under high Pressure. International Conference held in Leuven, Belgium, 1-5 September 1975. Edited by G. Thomas. (European Physical Society, Leuven, 1975) (Europhysics Conference Abstracts, vol. 1A) 81-82.

15. B. Buras and W.D. Ellenson, High Pressure Structural Transitions in C_6D_6 and $C_{10}D_8$. In: Risø Report No. 334 (1975) 36-37.

16. I. Heilmann (unpublished).

17. B. Buras and N. Niimura, Pressure-Volume Isotherms and the Critical Point in Ce-metal. Risø Report No. 352 (1976) 29-30.

18. P.S. Peercy and I.J. Fritz, Pressure-Induced Phase Transition in Paratellurite (TeO_2). Phys. Rev. Lett. 32 (1974) 466-469.

19. T.G. Worlton and R.A. Beyerlein, Structure and Order Parameters in the Pressure-Induced Transition in TeO_2. Phys. Rev. B 12 (1975) 1899-1907.

20. D.B. McWhan, R.J. Birgeneau, W.A. Bonner, H. Taub, and J.D. Axe, Neutron Scattering Study at High Pressure of the Structural Phase Transition in Paratellurite. J. Phys. C 8 (1975) L81-L85.

21. D.B. McWhan, D. Bloch, and G. Parisot, Apparatus for Neutron Diffraction at High Pressure. Rev. Sci. Instrum. 45 (1974) 643-646.

22. D.M. McWhan and I.M. Rice, Pressure Dependence of Itinerant Antiferromagnetism in Chromium. Phys. Rev. Lett. 19 (1967) 846-849.

23. H. Umebayashi, G. Shirane, B.C. Frazer, and W.B. Daniels, Neutron Diffraction Study of Cr under High Pressure. J. Phys. Soc. Japan 24 (1968) 368-372.

24. B.D. Rainford, B. Buras, and B. Lebech, Inelastic Neutron Scattering from Cerium under Pressure. Proceedings of the "International Conference on Magnetism", Amsterdam, The Netherlands, September 6-10, 1976. Physica B+C 86-88 (1977) 41-42.

ISBN 87-550-0456-3